A3310.—One kilogram of magnetite was mixed in an evaporating dish with 160 cc. of a solution of potassium silicate, which contained 0.249 gram of potassium oxide and 0.149 gram of silica per milliliter of solution. The mixture was treated with enough water to form a slurry which was evaporated nearly to dryness on a steam bath. The catalyst mass was then heated for 16 hours at 150° C. The material was sieved to the desired mesh size and divided into portions which were given different heat treatments. The sample that was given no further heat treatment was soft and magnetic. The sample that was further heated for 16 hours at 500° C. was hard and magnetic. The sample heated at 900° C. was hard but had become nonmagnetic, while the sample heated at 1,100° C. was soft and nonmagnetic.

A3811.—Reduced Scrub Oak magnetite glomerules were mixed with enough borax solution to furnish 5 percent borax. The mixture was evaporated to dryness on a steam bath, crushed, and sieved. It was necessary to add the glomerules to the solution under a flow of carbon dioxide to avoid oxidation of the catalyst by the atmosphere. After impregnation, the catalyst was rereduced before use in the synthesis.

CATALYSTS FROM COMMERCIALLY AVAILABLE SOURCES OF IRON

Because of the high cost of manufacturing precipitated and fused synthetic-ammonia-type catalysts, activity tests were made with catalysts prepared from relatively inexpensive materials. Readily available iron ores and industrial by-product iron oxides were prepared as described in table 20. Some of these preparations were bonded with alumina, as described in the previous section. The cemented forms had moderately high mechanical strength; however, the other materials were soft.

PHYSICAL PROPERTIES OF IRON CATALYSTS

An extensive discussion has already been presented on X-ray diffraction and thermomagnetic studies of ferric oxides and ferric oxide hydrates obtained by aging ferric salts or by precipitation from their solutions.[72] These studies have since been extended to include fused-, cemented-, and precipitated-iron catalysts. In addition, surface-area studies and pore-volume measurements have been made, especially to investigate the changes in these properties with reduction of the catalyst and with its use in the synthesis.

CRYSTAL STRUCTURE OF FUSED CATALYSTS

Lumps of fused catalyst were broken and powdered for precise determination of lattice parameters. The results (table 21) show that the lattice parameters decrease from 8.376 *kX*

[72] Work cited in footnote 71, p. 28.

TABLE 20.—*Catalysts from commercially available iron materials*

Catalyst	Materials			Preparation	Heat treatment
	Iron	Alkali	Others		
A1003	Crushed glomerules of magnetite.	None	None	Crushed to 6- to 10-mesh	None.
A2101.1 and A2101.2.	do	K_2CO_3	None	Impregnated with carbonate solution and evaporated to dryness with stirring.	16 hr. at 150° C.
A2103	Goethite ore α-$Fe_2O_3.H_2O$.	do	None	Crushed to 6- to 8-mesh; same as A2101.1.	Do.
L2014	Siderite, $FeCO_3$ by-product, Pennsylvania Salt Co.	do	None	Same as above	Same as above.
A3210	Pigment-grade Fe_2O_3	KNO_3	$Al(NO_3)_3$	Magnetite added to solution of $Al(NO_3)_3$ and KNO_3. Evaporated to dryness with stirring.	30 hr. at 150° C. 14 hr. at 900° C.
L3009	Mill scale	K_2CO_3	$Al(NO_3)_3$	Impregnated with $Al(NO_3)_3$ and evaporated to dryness with stirring. Crushed to size and impregnated with alkali and dried.	16 hr. at 150° C.
L2013	Alabama goethite ore.	do	None	Same as L2103	Same as L2103.
A3219	Magnetite from iron sulfate solution of pickling process.	KNO_3	$Al(NO_3)_3$	Same as A3210	Same as A3210.
A2104	Limonite ore	K_2CO_3	None	Same as A2103	Same as A2103.
A3312	Wrought-iron drippings.	do	None	do	Do.
A2300	Commercial ferrosilicon.	None	None	None	None.

TABLE 21.—*Lattice-constant measurements and chemical analyses of solid solutions of Al_2O_3 and MgO in Fe_3O_4*

Catalysts L2005, L2006, and L2007

Preparation No.	Catalyst No.	Content by preparation	Chemical analysis				Fe^{++}/Fe^{+++}	Spinel lattice constant, kX units [1]
			Fe^{++}	Fe^{+++}	MgO	Al_2O_3		
1	L2005	Pure fused iron oxide	25. 38	46. 67			0. 54	8. 3760
4		10 percent Al_2O_3	20. 99	43. 09		10. 24	. 48	
6		20 percent Al_2O_3	20. 19	36. 84		19. 38	. 55	
7	L2006	2.5 percent MgO	21. 79	48. 00	2. 19		. 45	8. 374
8		5 percent MgO	24. 98	43. 96	4. 14		. 57	8. 375
9		10 percent MgO	15. 90	48. 78	8. 87		. 33	8. 374
10		15 percent MgO	17. 38	43. 65	14. 06		. 40	8. 374
11		20 percent MgO	14. 75	43. 33	19. 02		. 34	8. 370
12	L2007	1.25 percent MgO, 1.25 percent Al_2O_3	25. 48	44. 80	1. 30	1. 53	. 57	
13		2.5 percent MgO, 2.5 percent Al_2O_3	23. 49	45. 23	2. 44	2. 77	. 52	
14		5 percent MgO, 5 percent Al_2O_3	20. 83	44. 18	3. 64	7. 02	. 47	
15		7.5 percent MgO, 7.5 percent Al_2O_3	18. 02	43. 26	6. 57	7. 41	. 42	
20		10 percent MgO, 10 percent Al_2O_3	17. 12	40. 47	10. 13	10. 66	. 42	
		Alan Wood magnetite concentrate	22. 90	48. 83		0. 1	. 47	8. 3775

[1] ± 0.002 kX unit.

units for pure magnetite to 8.370 kX units for a fused mixture of 20 percent magnesia and 80 percent magnetite. The latter value does not agree with that reported by Posnjak for magnesioferrite (20.3 percent magnesia), that in, 8.342 kX units.[73] That the magnesia was in solid solution was borne out by chemical analyses of these catalysts, as well as of similar preparations with magnesia and alumina, showing that the ratio of ferrous:ferric iron decreased with an increase in magnesia content.[74] This suggests that Mg^{++} replaced Fe^{++} in the spinel structure, so that the remaining Fe^{++} was less than half the amount of Fe^{+++} in the lattice. However, analysis of preparations made with alumina and no magnesia showed that Al^{+++} did not replace Fe^{+++} in the structure but probably formed γ-alumina, isomorphous with the magnetite spinel, and was incorporated into the catalyst structure as such. Failure of the lattice parameters to agree with those of Posnjak may be caused by inadequate annealing of the catalysts.

The unreduced catalysts produced sharp magnetite patterns; reduced catalysts, broad α-iron patterns. Sharp lines indicate large crystallites; diffuse lines indicate small crystallites. Reduced catalysts containing alumina or magnesia gave broader diffraction lines of α-iron than reduced pure magnetite, and the resistance to sintering of the catalysts containing structural promoter was attributed to the uniformly dispersed alumina or magnesia, which prevented the formation of large crystals. This hypothesis was supported by the fact that pure reduced magnetite is malleable, whereas reduced promoted catalysts are brittle.

[73] Posnjak, E., The Crystal Structure of Magnesium, Zinc, and Cadmium Ferrites: Am. Jour. Sci., vol. 19, 1930, pp. 67–70.

[74] Hofer, L. J. E. (unpublished data).

SURFACE AREAS AND PORE VOLUMES

FUSED-MAGNETITE CATALYSTS

Brunauer and Emmett studied the adsorption of nitrogen and of a number of other simple molecules, such as argon, methane, oxygen, carbon monoxide, carbon dioxide, and n–butane, at temperatures near the respective boiling points of the gases on reduced, promoted, and unpromoted synthetic-ammonia-type catalysts.[75–77]

Oxygen, carbon monoxide, and carbon dioxide isotherms were composites of physical and chemical adsorption. Table 22 shows the effect of promoters on the development of surface area of reduced synthetic-ammonia-type

[75] Brunauer, S., and Emmett, P. H., The Use of Low-Temperature van der Waals Adsorption Isotherms in Determining the Surface Areas of Various Adsorbents: Jour. Am. Chem. Soc., vol. 59, 1937, pp. 2682–2689.

[76] Emmett, P. H., and Brunauer, S., Accumulation of Alkali Promoters on Surfaces of Iron-Synthetic-Ammonia Catalysts: Jour. Am. Chem. Soc., vol. 59, 1937, pp. 310–315.

[77] Emmett, P. H., and Brunauer, S., The Use of Low-Temperature van der Waals Adsorption Isotherms in Determining the Surface Area of Iron-Synthetic-Ammonia Catalysts: Jour. Am. Chem. Soc., vol. 59, 1937, pp. 1553–1564.

TABLE 22.—*Surface areas of reduced iron synthetic-ammonia-type catalysts* [1]

Catalyst No.	Promoters, percent	Reduction and sintering conditions	Surface area,[2] $m.^2/gm.$
973I	0.15 Al_2O_3	124 hr. at 300°–500° C. plus 54 hr. at 375°–500° C	0. 38
973II	0.15 Al_2O_3	96 hr. at 300°–400° C	. 94
954I	10.2 Al_2O_3	48 hr. at 350°–450° C. plus 48 hr. at 450°–500° C	8. 38
931I	1.3 Al_2O_3+1.59 K_2O	18 hr. at 300°–350° C., 65 hr. at 350°–450° C., and 18 hr. at 450°–530° C.	3. 33
931II	1.3 Al_2O_3+1.59 K_2O	As I, plus sintering at 475° C	3. 01
931III	1.3 Al_2O_3+1.59 K_2O	As I, plus several partial oxidations and reductions at 450° C	2. 46
958	0.35 Al_2O_3; 0.08 K_2O	36 hr. at 350°–450° C. plus 36 hr. at 450°–500° C	1. 90
930	1.07 K_2O	48 hr. at 350°–450° C	. 43
424	1.03 Al_2O_3; 0.19 ZrO_2	Conditions not specified	7. 12

[1] From reference 77, p. 34.
[2] Surface areas per gram of unreduced catalyst as estimated by the B. E. T. point *B* method from nitrogen isotherms.

catalysts. The unreduced catalysts had very low surface areas; almost all of the surface area of reduced catalysts was developed during reduction. The postulate that alumina is a structural promoter in these catalysts was verified by X-ray diffraction data.[78] Although potassium oxide was not a structural promoter, activity data indicated that it enhanced the activity per unit of surface area of fused catalysts. Maxwell, Smart, and Brunauer[79] have recently reported magnetic evidence that alkali oxides form solid solution with magnetite in the unreduced catalyst.

Brunauer and Emmett believed chemisorption of carbon monoxide and carbon dioxide to be molecular and that of hydrogen and nitrogen to be atomic; they related the amount of chemisorbed gas to the amount of nitrogen adsorbed as a monolayer (table 23).[80] The physical adsorption of nitrogen gives an estimate of the total surface area, and the low-temperature (−183° C.) chemisorption of carbon monoxide indicates the fraction of the surface occupied by iron atoms. If it is assumed that carbon dioxide is adsorbed in a monolayer on only the potassium oxide surface (at −78° C.), an estimate may be made of the fraction of the surface occupied by each component of the catalyst. For example, in two singly promoted catalysts the aluminum oxide covered about 55 and 35 percent of the surface, respectively; about 70 percent of the surface was covered by the 1.07 percent of potassium oxide of a typical doubly promoted catalyst. Thus, promoters collect on the surface in greater quantities than in the bulk of the catalyst, a tendency that is greater for potassium oxide than for alumina.

These data agree with the observation that at least part of the alkali is volatilized from singly promoted catalysts and can be partly extracted from the raw catalyst with water and that the order of addition of alkali (before or after fusion) does not greatly change the

[78] Wyckoff, R. W. G., and Crittenden, E. D., An X-ray Examination of Some Ammonia Catalysts: Jour. Am. Chem. Soc., vol. 47, 1925, pp. 2866–2876.
[79] Maxwell, L. R., Smart, J. S., and Brunauer, S., Thermomagnetic Investigations of Promoted and Unpromoted Iron Oxide and Iron Catalysts: Jour. Chem. Phys., vol. 19, 1951, pp. 303–309.
[80] Brunauer, S., and Emmett, P. H., Chemisorption of Gases on Iron Synthetic Ammonia Catalysts: Jour. Am. Chem. Soc., vol. 62, 1940, pp. 1732–1746.

TABLE 23.—*Chemisorption on iron synthetic-ammonia-type catalysts* [1]

Catalyst No.	Promoters, percent	CO/N_2 monolayer [2]	CO_2/N_2 monolayer [3]	H_2 chemisorbed / CO chemisorbed [4]		N_2/CO [5]	N_2/N_2 monolayer [5]
				Type A, −78° C.	Type B, 100° C.		
973	0.15 Al_2O_3	1. 13	0. 13	0. 40	0. 41	0. 24	0. 35
954	10.2 Al_2O_3	. 43	. 05	. 57	. 59	. 34	. 15
424	1.03 Al_2O_3, 0.19 ZrO_2	. 65	. 08	----------	----------	----------	----------
930	1.07 K_2O	----------	. 74	----------	----------	----------	----------
931	1.30 Al_2O_3, 1.59 K_2O	. 44	. 61	. 94	. 95	. 50	. 26
958	0.35 Al_2O_3, 0.08 K_2O	. 62	. 27	. 50	----------	----------	----------

[1] From reference 80, above.
[2] Carbon monoxide chemisorbed at −183° C.
[3] Carbon dioxide chemisorbed at −78° C.
[4] Time of equilibration, 1 hour or longer.
[5] Nitrogen chemisorbed at 391°–395° C.

activity of the resulting catalyst. Thus, alumina is in solid solution in the magnetite, but potassium oxide does not appear to be very thoroughly incorporated in the raw catalyst. The magnetic evidence [81] cited above appears to contradict the latter conclusion. After reduction, the iron occupies less volume than the oxide from which it was formed, but the geometric volume of the catalyst remains essentially the same. Therefore, the iron atoms probably recede from the reduction zone, leaving a matrix of alumina. This alumina prevents the iron atoms from migrating to form structures of low surface area. The reduction of fused magnetite catalysts for the ammonia synthesis, as well as the properties of these catalysts, has been reviewed by Bokhoven, van Heerden, Westrik, and Zwietering.[82] A more general account of the reduction of magnetite and hematite has been given by Edström.[83]

The pore volumes and surface areas of raw fused-iron catalysts (measured at the Bureau of Mines) were very small (table 24), as was to be expected from the method of preparation. The pore volume of the precipitated catalyst (P3003.24) shown in this table was much greater than those of the fused or cemented catalysts; yet it was only 20 percent of the pore volume of a typical pelleted cobalt catalyst (89J).

STRUCTURAL CHANGES DURING REDUCTION OF FUSED CATALYSTS

In these studies [84] 6- to 8-mesh samples of catalyst D3001 and D3006 were used. The variation of the extent of reduction of catalyst D3001 at 450° with time is shown in figure 14. The circles represent the changes in a sample reduced progressively for adsorption studies, and the squares represent separate reductions of individual samples for pore-volume measurements. The good reproducibility justifies combining the two sets of data in calculating pore diameters as a function of the extent of reduction.

The upper curve of figure 15 (open circles) shows the surface area per gram of unreduced catalyst as a function of the extent of reduction at 450°. The surface area increased linearly with the extent of reduction to about 90 percent. Above this value, the slope decreases and becomes negative near 100-percent reduction. Point *a* corresponds to 99.4-percent reduction in 63 hours and points *b* and *c* to complete reduction in 85 and 116 hours, respectively. The curve just below this (open triangles) is a similar plot of the chemisorbed carbon monoxide per gram of unreduced catalyst. This curve also increases linearly up to about 85-percent reduction, beyond which point the curve bends sharply upward. This behavior is a characteristic that must be explained in any postulated reduction mechanism. The solid

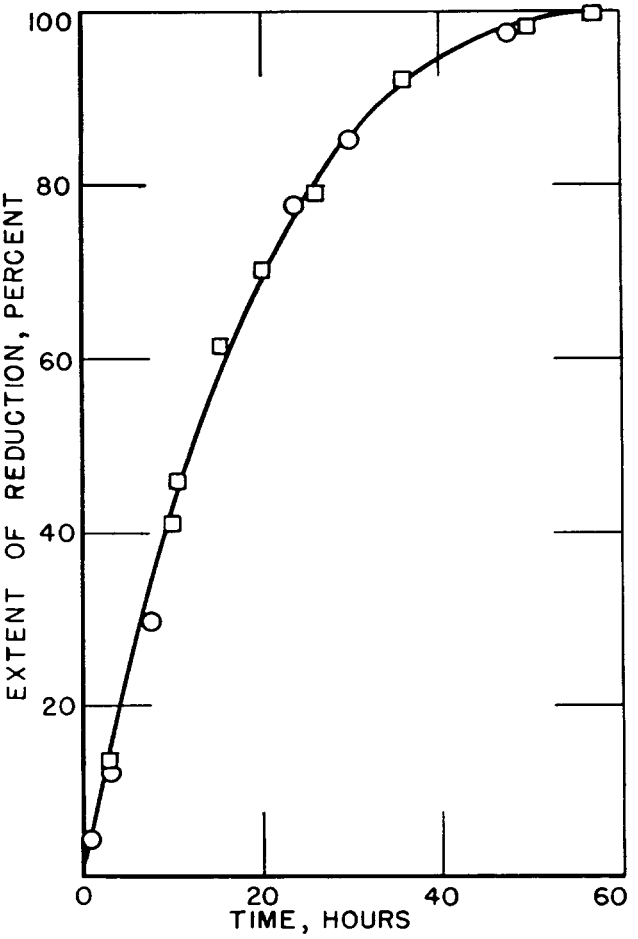

FIGURE 14.—Reduction of Catalysts D3001 at 450°C. and Hourly Space Velocity of 1,000 as a function of Time.

○, Data taken progressively on a single sample for surface-area measurements; □, independent determination on separate samples for pore-volume measurements.

[81] Work cited in footnote 79, p. 35.
[82] Bokhoven, C., van Heerden, C., Westrik, R., and Zwietering, P., Research on Ammonia Synthesis Since 1940: Chap. 7, Catalysis, vol. III (ed. P. H. Emmett), Reinhold Publishing Corp., New York, N. Y., 1955, pp. 265–348.
[83] Edström, J. O., The Mechanism of Reduction of Iron Oxide: Jour. Iron and Steel Inst., vol. 175, 1953, pp. 289–304.
[84] Hall, W. K., Tarn, W. H., and Anderson, R. B., Studies of the Fischer-Tropsch Synthesis. VII. Surface Area and Pore-Volume Studies of Iron Catalysts: Jour. Am. Chem. Soc., vol. 72, 1950, pp. 5436–5443.

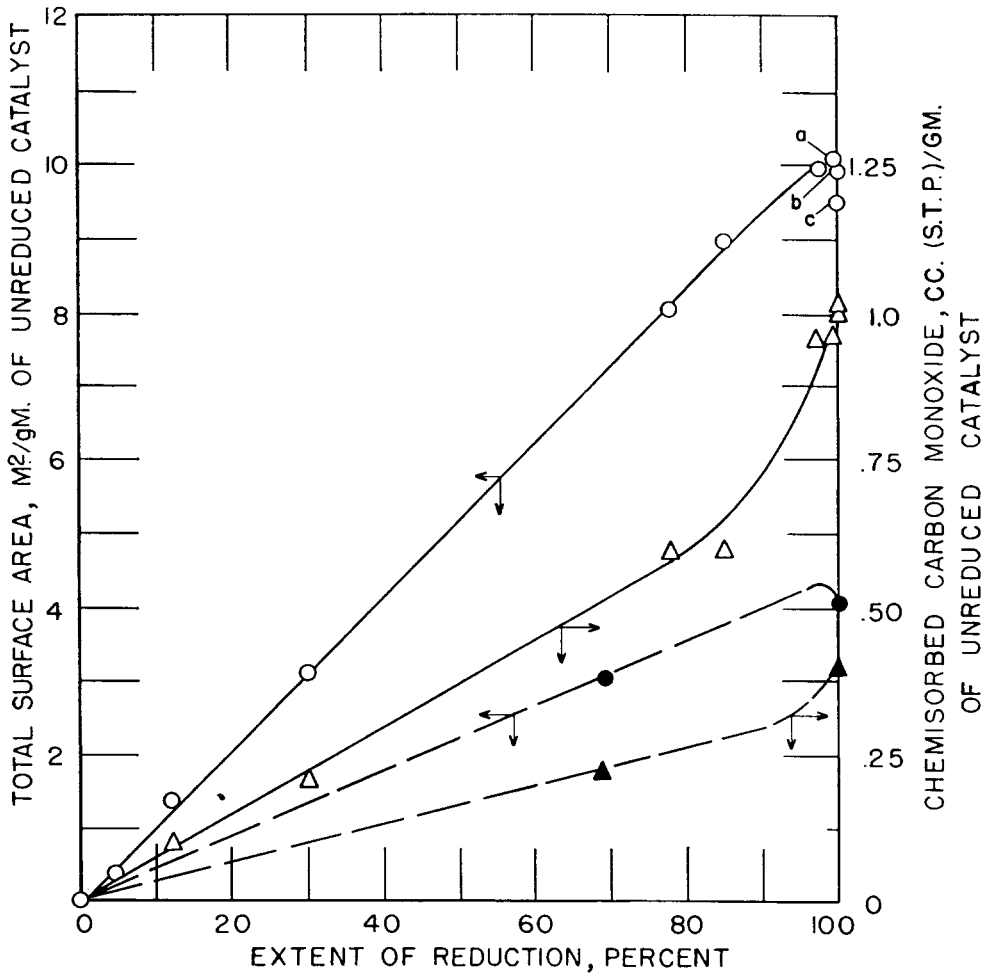

FIGURE 15.—Variation of Surface Area and of Carbon Monoxide Chemisorption With Extent of Reduction.

○, Surface area of samples reduced at 450° C.; △, corresponding chemisorption of carbon monoxide; solid points, samples reduced at 550° C.

TABLE 24.—*Comparison of physical properties of raw (unreduced) fused-, cemented-, and precipitated-iron catalysts at 30° C.*

Catalyst No.	Type	Composition	Mesh size	d_{He}, cc./gm.	d_{Hg}, cc./gm.	Pore volume, cc./gm.	Surface area m.²/gm.
A1000	Fused	Fe_3O_4	8–14	5. 33	5. 24	0. 003	(1)
D3001	do	Fe_3O_4–MgO–K_2O	6–8	4. 96	4. 91	. 002	~0. 01
D3004	do	Fe_3O_4–Al_2O_3–K_2O	6–8	4. 98	4. 89	. 003	~. 01
D3008	do	Fe_3O_4–Al_2O_3–K_2O	6–14	5. 10	4. 99	. 004	(1)
A3310	Cemented	Fe_3O_4–K_2SiO_3	6–8	4. 74	3. 48	. 076	~. 1
A3213.24	do	Fe_3O_4–Al_2O_3–K_2O	6–8	5. 02	3. 81	. 063	1. 4
L1002.2	do	Fe_3O_4–$Na_2B_4O_7$	6–8	4. 99	3. 46	. 089	~. 1
A. W. magnetite [2]		Fe_3O_4	4–10	5. 14	3. 43	. 097	~. 6
P3003.24	Precipitated	Fe_2O_3–CuO–K_2CO_3	6–8	4. 43	2. 83	. 125	184
89J	do	Co–ThO_2–MgO–KG	(3)	2. 76	. 974	. 66	88. 7

[1] Not determined. Very probably about 0.01 m.²/gm.
[2] Soft granules formed by mixing the powder with water and drying.
[3] Pellets, ⅛ in.×1/16 in.

TABLE 25.—*Density and adsorption data of catalyst D3001 as a function of extent of reduction* [1]

Reduction, percent	d_{He}, cc./gm.	d_{Hg},[2] cc./gm.	Volume[3] of Hg displaced, cc./gm. unreduced catalyst	Pore[4] volume, cc./gm. unreduced catalyst	$\bar{d}$,[5] A.	Surface area, m.²/gm. unreduced atalyst	V_m,[6] (NTP) cc./gm.	V_{CO},[7] (NTP) cc./gm.	$\frac{V_{CO}}{V_m}$
0.0	4. 96	4. 91	0. 203	0. 002		0. 0	0. 0	0. 0	
10.0	5. 07	. 80	. 203	. 010	400	1. 0	. 23	. 09	0. 39
20.0	5. 18	4. 68	. 203	. 018	343	2. 1	. 48	. 16	. 33
30.0	5. 32	4. 56	. 203	. 027	348	3. 1	. 71	. 22	. 31
40.0	5. 45	4. 45	. 202	. 035	333	4. 2	. 96	. 29	. 30
50.0	5. 60	4. 33	. 204	. 043	331	5. 2	1. 29	. 36	. 28
60.0	5. 77	4. 22	. 201	. 052	330	6. 3	1. 44	. 43	. 30
70.0	5. 98	4. 10	. 200	. 061	334	7. 3	1. 67	. 50	. 30
80.0	6. 22	3. 98	. 200	. 071	338	8. 4	1. 92	. 57	. 30
90.0	6. 50	3. 87	. 199	. 082	349	9. 4	2. 15	. 67	. 31
95.0	6. 65	3. 81	. 199	. 086	348	9. 9	2. 26	. 83	. 37
100.0	6. 82	3. 75	. 198	. 089	352	10. 1	2. 31	1. 00	. 43
100.0 [8]	6. 82	3. 78	. 197	. 088	371	9. 5	2. 20	1. 00	. 45
100.0 [9]	6. 95	3. 71	. 201	. 094	917	4. 1	. 94	. 38	. 40
68.9 [9]					832	3. 1	. 71	. 22	. 31
KCl [10]	1. 983	1. 978		. 000					
	1. 984								

[1] All reductions were made with a flow of 1,000 volumes of pure H_2 gas per volume of catalyst space per hour and at 450° C., except where otherwise noted. The catalyst was in all instances 6- to 8-mesh.

[2] Determined at an absolute pressure of 1,100 mm. Hg.

[3] $V_x=(1-f)d_x$, where d_x is the helium or mercury density and f is the fractional weight loss on treatment.

[4] Difference between the volume of Hg and He displaced.

[5] $\bar{d}=\frac{4\text{ (pore volume.)}}{\text{Surface area}}$

[6] Volume of nitrogen corresponding to a monolayer, per gram of unreduced catalyst.

[7] Volume of carbon monoxide chemisorbed at −195° C. per gram of unreduced catalyst.

[8] This row of data was obtained on a sample reduced for 116 hours at 450° C.

[9] These data were obtained on samples reduced at 550° C.

[10] KCl was used to check our calibrations; observed values are shown in the upper row, and literature value is below.

circles and triangles found in the lower 2 curves present similar data for samples of this catalyst reduced at 550° C. and show the general effects of changing the reduction temperature.

The experimental density data are plotted in figure 16. The density and adsorption data in table 25 have been taken from the curves in figures 15 and 16. In figure 17, however, which shows the pore volume as a function of the extent of reduction, actual experimental points have been plotted. Column 4 of table 25 lists volumes of mercury displaced by reduced catalysts per gram of unreduced material. These volumes are essentially the same for all extents of reduction, which is interpreted as indicating that the external volume of the catalyst particle does not change during reduction and that mercury does not penetrate any of the pores. This explanation was substantiated by the observation that the linear dimensions, by direct measurement, of polished pieces of catalyst before and after reduction remained constant.

The average pore diameters in table 25 were calculated on the basis of cylindrical open-end pores by the equation of Emmett and DeWitt.[85] From 20- to 95-percent reduction, $\bar{d}$ varied from 330 to 348 A. but increased to 371 A. as the reduction approached 100 percent. The value of $\bar{d}$ for 10-percent reduction may be regarded as somewhat uncertain, because both the surface area and the pore volume are small. It has been shown [86] that this pore diameter must be considered as an upper limit of the real diameter.

The variation of surface area and pore volume with reduction temperature for completely reduced samples of catalysts D3001 and D3006 is shown in table 26. The pore volumes and the volumes of mercury displaced by the reduced samples per gram of unreduced catalyst remained essentially constant, whereas the surface area decreased from 9.4 to 1.6 m.²/gm., and the average pore diameter decreased from 2,420 to 366 A. as the temperature of reduction was increased from 450° to 650°. The ratio V_{co}/V_m was essentially constant at about 0.3 for the D3006 series. This value was lower than those of the completely reduced D3001 samples.

A simple explanation of the changes that occur in the reduction of fused-iron catalysts involves the following premises: (1) The external volume of the particles does not change in the reduction; the pore structure of the

[85] Emmett, P. H., and DeWitt, T. W., The Low-Temperature Adsorption of Nitrogen, Oxygen, Argon, Hydrogen, n-Butane, and Carbon Dioxide on Porous Glass and on Partially Dehydrated Chabazite: Jour. Am. Chem. Soc., vol. 65, 1943, pp. 1253-1262.

[86] Anderson, R. B., and Hall, W. K., Modifications of the Brunauer, Emmett, and Teller Equation. II: Jour. Am. Chem. Soc., vol. 70, 1948, pp. 1727-1734.

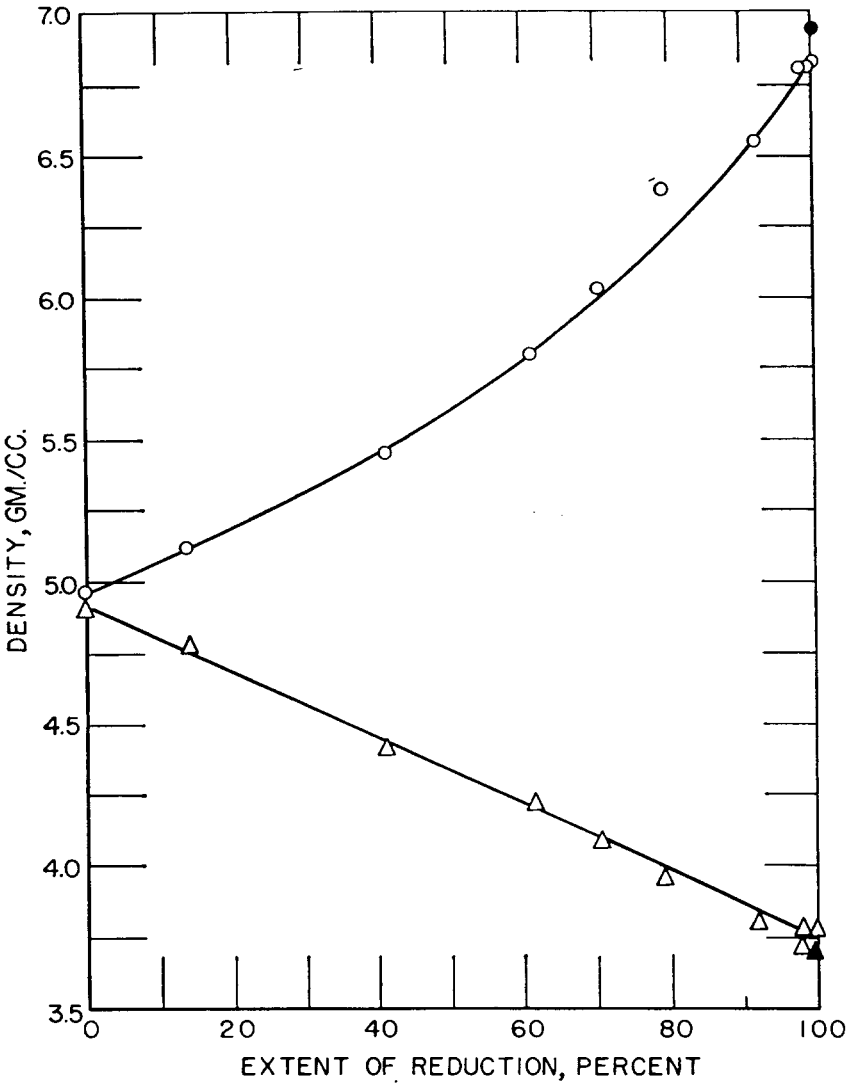

FIGURE 16.—Variation of Mercury and Helium Densities With Extent of Reduction.

○, absolute densities of catalysts reduced at 450° C. measured by displacement of He; △, corresponding densities measured by displacement of Hg; solid points, samples reduced at 550° C.

TABLE 26.—*Density and adsorption data of synthetic-ammonia-type catalysts as a function of reduction temperature* [1]

Catalyst	Reduction temp.,[2] ° C.	V_m, cc. (STP)/gm.	V_{co}, cc. (STP)/gm.	$\frac{V_{co}}{V_m}$	Surface area, m.²/gm.	Volume of Hg displaced, cc./gm.	Pore [3] volume, cc./gm.	$\overline{d}$,[4] A
D3001	450	2. 31	1. 00	0. 43	10. 1	0. 198	0. 089	371
D3001	550	. 94	. 38	. 40	4. 1	. 201	. 094	917
D3006	450	2. 15	. 72	. 34	9. 4	. 194	. 086	366
D3006	500	1. 21	. 42	. 35	5. 3	. 198	. 091	687
D3006	550	1. 02	. 32	. 31	4. 5	. 195	. 090	800
D3006	600	. 46	. 10	. 22	2. 0	. 193	. 092	1, 840
D3006	650	. 38	. 12	. 32	1. 6	. 199	. 097	2, 420
D3006 [5]						. 201		

[1] All data given in terms of grams of unreduced catalyst.
[2] The D3006 samples were 4-to-6-mesh reduced in pure, dry H_2 flowing at a rate of 2,000 volumes of gas per volume of catalyst space per hour.
[3] Difference between the volume of Hg and He displaced.
[4] $\overline{d}=4$ (pore volume)/surface area.
[5] This was an unreduced sample.

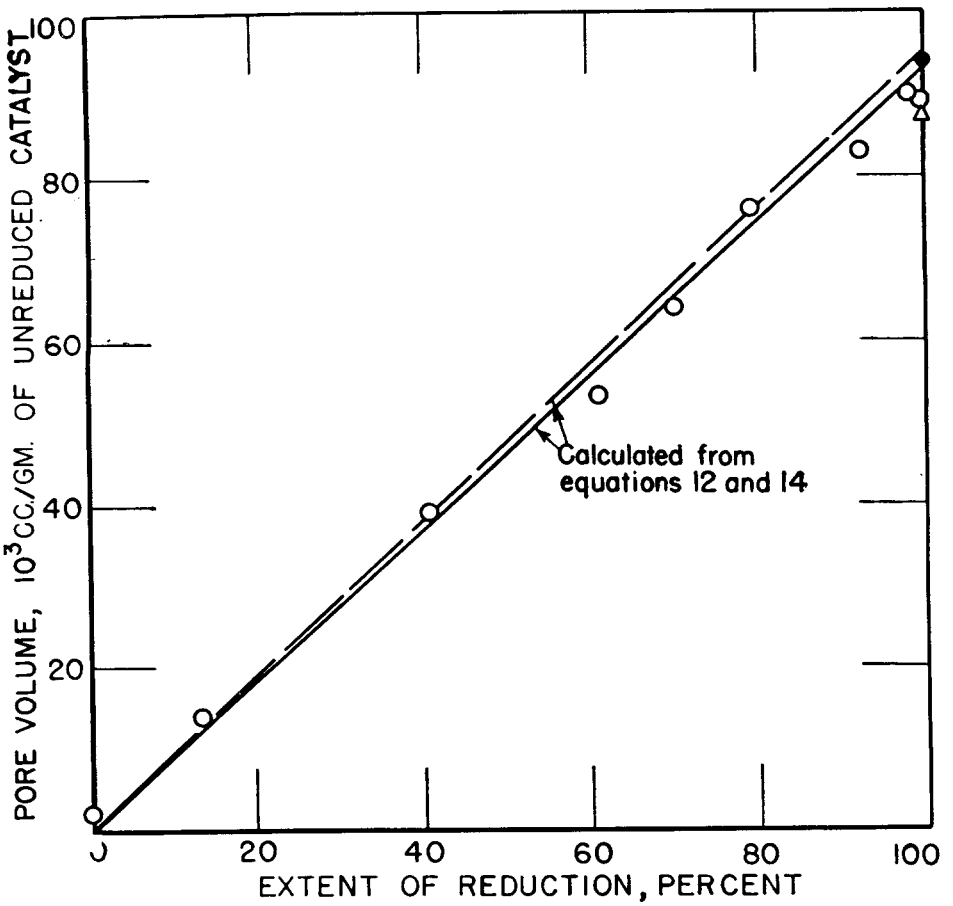

FIGURE 17.—Variation of Pore Volume per Gram of Unreduced Catalyst With Extent of Reduction of Catalyst D3001.

○, reduction at 450° C.; ●, reduction at 550° C.; and △, 115-hour reduction and sintering at 450° C.

catalyst is produced by the removal of oxygen. (2) Once initiated in a portion of the catalyst, the reduction proceeds very rapidly in that portion nearly, but not quite, to completion. The reduction proceeds directly from Fe_3O_4 to Fe, which is in accord with thermodynamic data.[87] (3) At 450° the reduced portion is quickly transformed to a relatively stable structure with an average pore diameter of 330 A. (4) On a macroscopic scale the reduction begins at the surface and moves uniformly inward. The rate data in figure 14 (p. 36) are satisfactorily approximated by an equation derived for spherical particles, assuming that the reduction proceeds uniformly inward from the external surface and that the rate is proportional to the area of the sphere of unreduced catalyst (see p. 45). The mechanism is substantiated by the photographs of polished sections of partly reduced particles of magnetite of Udy and Lorig.[88] These demonstrated that the Fe–Fe_3O_4 interface moved uniformly inward with the time of reduction.

On the basis of premises 1 and 2, the pore volume should increase linearly with the extent of reduction (fig. 17). Up to 90-percent reduction the surface area also increased linearly (fig. 15), indicating the formation of pores of constant diameter. This predicts that a plot of surface area against pore volume should be linear, as shown in figure 18. The slope of the linear portion of the curve corresponds to an average diameter of 333 A. At reductions greater than 80 percent the average pore diameter increases, since the surface area increases less rapidly than the pore volume.

From premises 1 and 2 it is apparent that calculation of the pore volume at any extent of reduction is possible if the initial and final densities are known. Consider 1 gram of unreduced material composed of Fe_3O_4 and inert (unreducible) material. On reduction, part of the oxide changes to metallic iron and

$$\text{Pore volume} = V_o - V_x, \qquad (11)$$

[87] Ralston, O. C., Iron Oxide Reduction Equilibria, a Critique From the Standpoint of the Phase Rule and Thermodynamics: Bureau of Mines Bull. 296, 1929, 326 pp.

[88] Udy, M. C., and Lorig, C. H., The Low-Temperature Gaseous Reduction of a Magnetite: AIME, Tech. Pub. 1509, 1942, 19 pp.

where V_0 is the initial volume per gram and V_x the actual (helium) volume per gram of unreduced material after reduction to some fraction, f, of complete reduction. If the volume contributions of the constituents are additive,

$$V_x = \sum_{\substack{\text{all}\\\text{phases}}} V_i = \sum_{\substack{\text{all}\\\text{phases}}} m_i/d_i. \quad (12)$$

where V_i, m_i, and d_i are the volume and mass per gram of unreduced catalyst and the absolute density, respectively, of component i. The volumes of iron and magnetite may be evaluated in terms of the initial and final volumes of the catalyst V_0 and V_F, respectively, and if the volume of the unreducible portion is V_b, then

$$V_x = (V_F - V_b)f + (1-f)(V_0 - V_b) + V_b$$
$$= V_0 + (V_F - V_0)f, \quad (13)$$

and from equations (11) and (13)

$$\text{Pore volume} = (V_0 - V_F)f. \quad (14)$$

The solid line in figure 17 is a plot of equation (14), with V_0 and V_F evaluated from helium densities of the original and the completely reduced catalyst. The agreement with the experimental data is satisfactory. It is also possible, however, to compute V_0 and V_F from the density of the phases present in the catalyst and from their weight fractions by equation (12). The dashed line in figure 17 was determined in this manner.

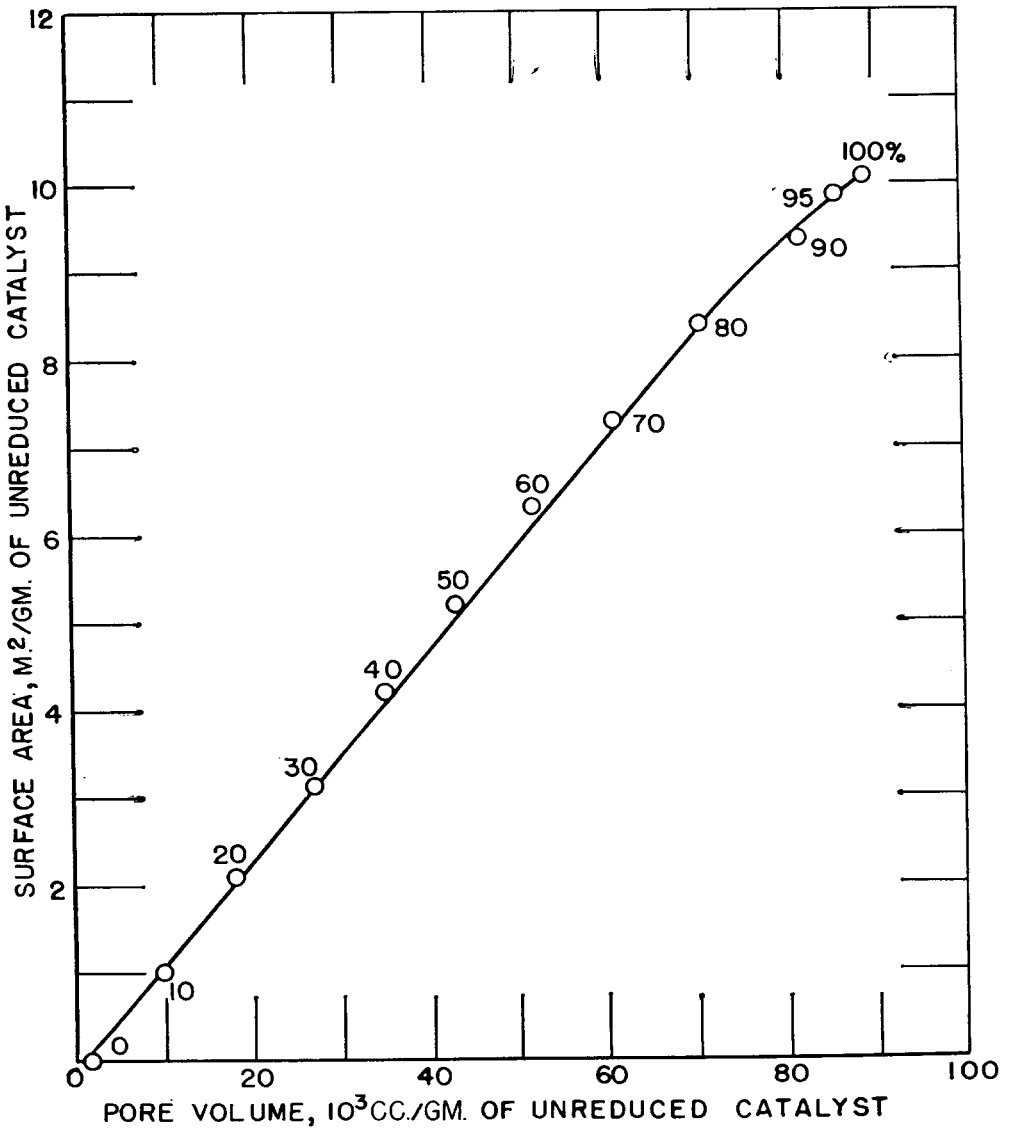

FIGURE 18.—Variation of Surface Area With Pore Volume.
Numbers on curve indicate extent of reduction.

466782°—59——4

The increase in the ratio of chemisorbed carbon monoxide to the nitrogen monolayer as the reduction nears completion may result from removal of the last portions of residual iron oxide from the "reduced" part of the catalyst. Between 99.5- and 100-percent reduction, where the slope of the chemisorbed carbon monoxide curve was the greatest, about 1 additional carbon monoxide molecule was chemisorbed for every 100 iron atoms produced. The surface area of the catalyst decreased in this range, and the data suggest that the residual iron oxide may act as a structural promoter. This decrease may also be attributed, however, to sintering during the long reduction period. The significant fact is, nevertheless, that the decrease in surface area occurs simultaneously with the increase in the V_{CO}/V_m ratio.

The effect of increasing the reduction temperature from 450° to 550° on catalyst D3001 is shown in figure 15 (p. 37). At 550° the reduced portion is transformed to a stable structure with an average pore diameter of 830 A, about 2.5 times the diameter of the 450° reduction. At about 70-percent reduction, the ratios of V_{CO}/V_m are nearly identical for both temperatures of reduction.

The external volume of the particles of D3006 (table 26) also remained unchanged in reductions at temperatures up to 650°. However, the surface area decreased sizably as the reduction temperature increased, and as the pore volume remained essentially constant, the average pore diameter varied in an inverse manner. Reduced, pure, fused magnetite has a low surface area, about 1.0 m.^{2} per gm., when reduced at 376°. The presence of structural promoters—MgO, SiO_2, and possibly Cr_2O_3—in catalysts D3001 and D3006 stabilized the surface formed in the reduction, so that moderately high surface areas were attained at reduction temperatures as high as 650°. The presence of these promoters, however, does not prevent a decrease in area with increasing temperature of reduction. For catalysts of this type variation of the temperature of reduction affords a method of "tailormaking" catalysts of any desired pore diameter over a relatively wide range. As the pore volume can be computed from equation 14, calculation of the average pore diameter requires only determination of the surface area.

PRECIPITATED-IRON CATALYSTS

Effect of Pretreatment on Structural Properties

Iron catalysts were examined by means of the electron microscope in a series of studies similar to those reported for cobalt catalysts.[89] Iron-copper-potassium carbonate (100:10:0.5) catalyst was prepared by the method described in the section on catalyst preparation. Figure 5, micrograph *18*, shows that this unreduced iron oxide catalyst has the structure of unpromoted ferric oxide gel (fig. 1, micrograph *1*). After the usual induction procedure[90] ($1H_2$:1CO, 24 hours, 230° C., 100 SVH), the catalyst was reduced to a mixture of magnetite and Hägg carbide (fig 5, micrograph *19*). The surface area was thereby decreased from 303 to 23 m.^{2} per gm. (table 6).

Previous work has indicated that unreduced, precipitated iron catalysts have gellike structures with pores of small diameter and large surface areas of 100 to 250 m.^{2} per gm.[91] A comparison of these properties of precipitated catalyst P3003.24 with those of cemented catalysts and fused catalysts is given in table 24. Precipitated catalyst P3003.24 had a considerably higher surface area than any fused or cemented catalyst.

Reduction of typical unpromoted iron catalysts 10K and 47C in hydrogen decreased the surface area to only 8 percent of the original area. When a sample was inducted with synthesis gas ($1H_2$:1CO) at atmospheric pressure and 325° C. for 24 hours, similar sintering occurred, and treatment with hydrogen at 325° C. after this induction caused no change in surface area. Data for these experiments are shown in table 27.

It was desirable to determine whether these changes in surface area resulted wholly or partly from thermal sintering or during reduction of the catalyst and to characterize the pore structure of precipitated-iron catalysts as they are used in the synthesis. Accordingly, samples of precipitated catalyst P3003.24 (100Fe:10Cu:0.5K_2CO_3) were heated in nitrogen at different temperatures, and other samples were reduced in hydrogen at 300° C.; the surface areas and mercury and helium densities were then determined.[92]

Data for nitrogen adsorption measurements at −195° are presented in figure 19 and table 28. The isotherms in figure 19 show that the average pore diameter increased rapidly [93] and the surface area decreased as the catalyst was sintered in nitrogen at increasing temperatures. Isotherms of samples sintered at temperatures

[89] McCartney, J. T., Seligman, B., Hall, W. K., and Anderson, R. B., An Electron-Microscopic Study of Metal Oxides and Metal Oxide Catalysts: Jour. Phys. and Colloid Chem., vol. 54, 1950, pp. 505–519.

[90] Storch, H. H., Anderson, R. B., Hofer, L. J. E., Hawk, C. O., Anderson, H. C., and Golumbic, N., Synthetic Liquid Fuels From Hydrogenation of Carbon Monoxide, Part I.: Bureau of Mines Tech. Paper 709, 1948, 213 pp.

[91] Work cited in footnote 90.

[92] Work cited in footnote 84, p. 36.

[93] This is inferred from the Kelvin equation

$$\ln \frac{p}{p_0} = \frac{-2\sigma V \cos \theta}{r RT},$$

where σ is the surface tension, θ is the contact angle, V is the molar volume, R is the gas constant, T is the absolute temperature, r is the pore radius and p/p_0 is the relative pressure corresponding to the steepest part of the desorption isotherm. Everything else being constant, r decreases as p/p_0 increases (see footnote 27, p. 7).

TABLE 27.—*Changes in the surface area of catalyst* $10K(Fe_2O_3-K_2CO_3)$ *on induction and reduction*

All data based on weight of raw catalyst

Sample	Treatment			Total weight loss, percent	Surface area, $m.^2/gm.$	V_m nitrogen, cc./gm.	Volume of chemisorbed CO, cc./gm.
	Gas	Temp., ° C.	Time, hours				
a [1]				0. 0	169. 1	38. 6	0. 0
b	(*a*) + $1H_2 : 1CO$	325	24	10. 3	12. 3	2. 8	. 6
c	(*b*) + H_2	325	16	12. 9	12. 0	2. 7	
d	(*c*) + H_2	325	16	15. 5	12. 1	2. 8	. 4
e	(*a*) + H_2	250–360	8	8. 2	9. 0	2. 1	
		360	2				

[1] Untreated catalyst.

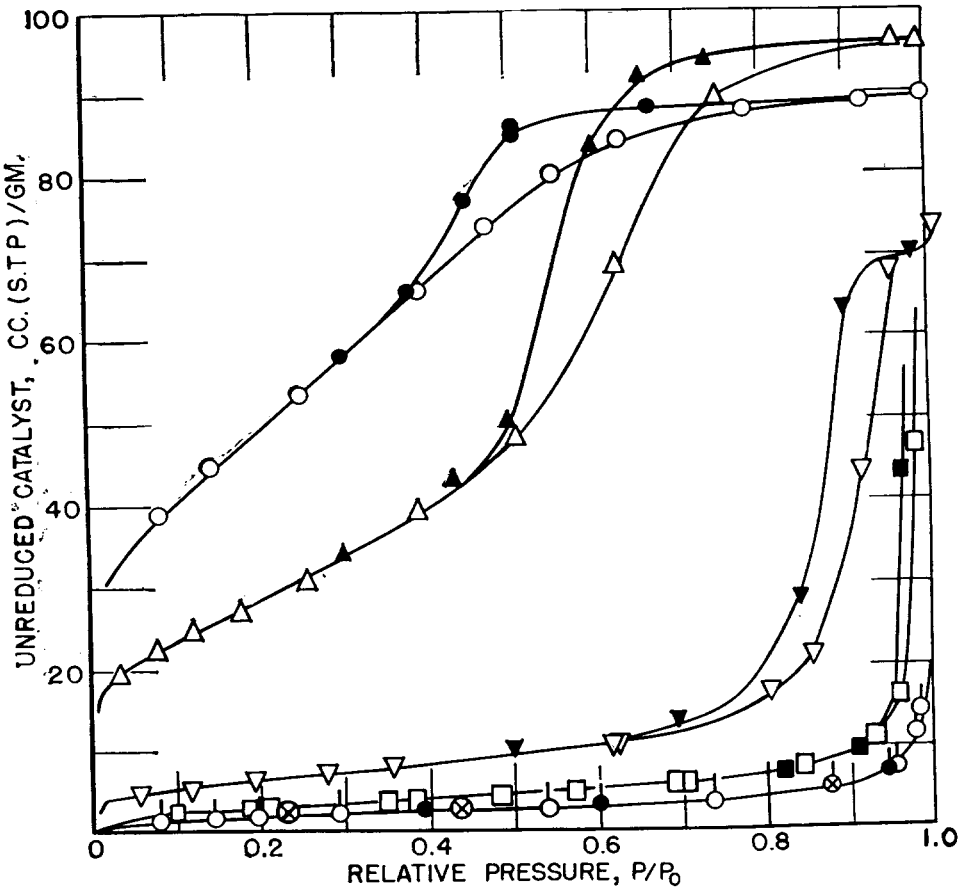

FIGURE 19.—Nitrogen-Adsorption Isotherms of Catalyst P3003.24 at −195° C. After Heat Treatment and Reduction.

○, After evacuation at 100° C.; △, after heating in N_2 at 300° C.; ▽, after heating at 450° C.; ⊗, after heating at 550° C.; □, after conversion to Fe_3O_4 by reduction at 250° C. with H_2 saturated with H_2O vapor; ◇, after heating at 300° C. followed by reduction with H_2 at 300° C.; adsorption points open, desorption points solid.

up to 450° were type IV of Brunauer's classification,[94] and those of samples sintered at higher temperatures or reduced in hydrogen were type II. Reduction to magnetite or iron (samples 6 and 5) produced about the same large change in the isotherm as sintering at 550°. Experiments were made to determine whether the glow phenomenon [95] occurred when the catalyst was heated in air to 550°, but results were inconclusive. X-ray diffraction patterns of the

[94] Brunauer, S., The Adsorption of Gases and Vapors: Physical Adsorption, Princeton Univ. Press, Princeton, N. J., 1943, p. 150.

[95] Weiser, H. B., Inorganic Colloid Chemistry, vol. II: John Wiley & Sons, New York, N. Y., 1935, p. 22.

TABLE 28.—*Isotherm data of heat-treated and reduced precipitated catalyst P3003.24*

Sample	Treatment				Type of isotherm [1]	Surface area, m.²/gm. of unreduced catalyst	V_s[2], cc. of liquid N_2/gm. unreduced catalyst
	Gas	Temp., ° C.	Time, hours	Weight loss, percent			
1	Evac	100	1	1. 7	IV	184. 0	0. 140
2	N_2	300	16	5. 0	IV	97. 4	. 150
3	N_2	450	16	5. 9	IV	23. 4	. 110
4	N_2	550	16	6. 4	II	8. 4	
5 [3]	H_2	300	17	[4] 33. 0	II	6. 3	
6	H_2–H_2O [5]	250	19	9. 2	II	11. 3	

[1] See reference 94, p. 43.
[2] Nitrogen adsorbed at p_o.
[3] Sample after treatment 2.
[4] Sum of 2+5.
[5] H_2 gas was saturated with H_2O at 26°.

treated materials showed those sintered in nitrogen to be Fe_2O_3, those reduced in hydrogen saturated with water vapor to be Fe_3O_4+Cu, and those reduced with pure dry hydrogen to be mainly α–Fe and Cu, with some residual Fe_3O_4.

The samples used to obtain the density measurements shown in table 29 were treated in the same way as those in table 28. The helium densities increased toward the calculated density of a mixture of hematite and copper oxide (5.21) as the temperature of sintering was increased. The helium density of the sample reduced with hydrogen containing water vapor was 5.25 compared with 5.35 for a mixture of magnetite and copper. Reduced sample 11 had a density of 7.60 compared with 7.98 for a calculated mixture of iron and copper.

The volume of mercury displaced per gram of unreduced catalyst (column 8, table 29) decreased with increasing sintering temperature. Reduction to magnetite caused about the same decrease in this volume as heating in nitrogen at the same temperature, but reduction to iron in dry hydrogen caused a greater decrease in volume than heat treatment in nitrogen at 550°. The decrease in the volume of mercury displaced may result from a decrease in the bulk volume of the particles or from the formation of pores large enough to permit penetration by mercury. The former is probably the most important effect, as the bulk volume of the catalyst was observed to decrease in treatments with nitrogen or hydrogen. The pore volumes obtained as the difference between the volume of helium and the volume of mercury displaced were in general agreement with those computed from the flat upper portions of the type IV isotherms, with the assumption that the adsorbed nitrogen has the same density as normal liquid. The pore volume increased when the catalyst was heated in nitrogen to 300° but decreased as the catalyst was heated to higher temperatures. The first increase was probably

TABLE 29.—*Mercury and helium densities, pore volumes, and pore diameters of catalyst P3003.24*

Sample	Treatment				d_{Hg},[1] cc./gm.	d_{He}, cc./gm.	Volumes displaced,[2] cc./gm. of unreduced catalyst		Pore volume,[3] cc./gm. of unreduced catalyst	Pore diameter, $\bar{d}$, A
	Gas	Temp., ° C.	Time, hours	Weight loss, percent			V_{Hg}	V_{He}		
7	Evac	100	1	1. 6	2. 83	4. 43	0. 347	0. 222	0. 125	27
8	N_2	300	16	5. 5	2. 79	4. 84	. 388	. 196	. 151	59
9	N_2	450	16	6. 1	3. 14	5. 04	. 299	. 186	. 113	193
10	N_2	550	16	6. 5	3. 20	5. 11	. 293	. 183	. 109	519
11	H_2	300	17	32. 6	2. 73	7. 60	. 247	. 089	. 155	968
12	H_2–H_2O	250	18	12. 7	2. 75	5. 25	. 317	. 166	. 151	536

[1] Determined at an absolute pressure of 1,100 mm.
[2] $V_x=(1-f)/d_x$, where d_x is the helium or mercury density, and f is the ractional weight on treatment.
[3] Difference between the volume of Hg and He displaced.
[4] $\bar{d}=4$ (pore volume)/surface area; surface area obtained from table 28.

due to the removal of water accompanied by only slight sintering of the pore structure, but at 450° considerable sintering of the pore structure occurred. At 550°, and to an even greater extent in the reductions, the pore structure is drastically altered. After reduction in dry hydrogen, the pore volume was increased to 0.155 cc. per gm., a value greater than that of the original catalyst. The average pore diameter in table 29 increased by a factor of 35, in agreement with the shapes of the isotherms in figure 19.

The detailed surface-area and pore-volume data obtained for two types of iron Fischer-Tropsch catalysts show that the surface areas and pore volumes of fused catalysts are created in the reduction, whereas precipitated catalysts initially have large surface areas that decrease as reduction proceeds. Although these types of catalysts are vastly different in the raw state, after reduction their surface areas and pore volumes are very similar. Precipitated catalyst P3003.24 is principally a ferric oxide gel. When heated in nitrogen at 300° the sample lost water, and the pore volume increased. Heating in nitrogen at higher temperatures caused only a slight additional decrease in weight but caused the pore volume to decrease from the maximum value observed at 300°. The surface area decreased progressively as the temperature of sintering was increased. As the changes in pore volume were relatively small with respect to the decrease in surface area, the average pore diameter increased monotonically with increasing sintering temperature. When the sample was reduced only to magnetite at 250° in hydrogen saturated with water vapor at room temperature, the pore volume increased, whereas the surface area decreased about as much as that observed in sintering at 550°. The ferric oxide gel is much more stable to thermal sintering than to reduction. Presumably reduction, even to magnetite, causes a major reorientation of the structural geometry. Reduction to iron at 300° caused a greater decrease in area, and again the pore volume increased. The volume of the particles, as indicated by the volume of mercury displaced, decreased in all sintering or reduction steps, the greatest change being observed in the sample reduced to iron. The sintering of ferric oxide gel catalysts during reduction is of significance to the Fischer-Tropsch synthesis, because these catalysts are reduced, at least to magnetite, either in pretreatment or in the subsequent synthesis.

Effect of Method of Preparation.

In preparing 100Fe : 10Cu : $0.5K_2CO_3$ precipitated catalysts in large batches, it was observed that some preparations were glossy black, like the small batches, while others were brown and much less glossy. Table 30 shows adsorption data for both types of unreduced catalysts before and after their induction at 230° in $1H_2 : 1CO$ gas. Chemisorption of carbon monoxide at −195° C. was determined after induction and is a measure of the fraction of iron present on the catalyst surface. Both raw catalysts had large surface areas and small pores. The black catalyst contained more water per gram than the brown. The decrease of the surface areas of both catalysts on induction is consistent with other data on the change in surface area of gel-type iron catalysts. The isotherm of the black catalyst (fig. 20) was of the type observed for some silica gels; but that of the brown catalyst was unusual, being linear from relative pressures of 0.1 to 0.7. Both isotherms showed hysteresis.

TABLE 30.—*Physical properties of Fe:Cu:K_2CO_3 catalysts*

Catalyst	Before induction		After induction in $1H_2$:1CO gas at 230° C.			
	Surface area,[1] m.²	Average pore diameter,[2] A.	Weight loss, percent	Surface area,[1] m.²	Volume CO chemisorbed,[1] cc.	V_{co} chemisorbed / V_m, N_2
Black: P3003.03	303	28.0	10.3	22.9	0.93	0.18
P3003.042[3]						
P3003.05						
Brown: P3003.07	135	41.6	5.9	15.5	.70	.20

[1] Per gram of unreduced catalyst.

[2] Calculated by the formula $d=\frac{4V_1}{A}$ where A is the surface area and V_1 the volume adsorded at 0.98 relative pressure computed as liquid.

[3] Composite sample.

CEMENTED CATALYSTS

Mercury- and helium-density measurements showed that raw, cemented-iron catalysts have considerably larger pore volumes and surface areas than the raw, fused-iron, synthetic-ammonia-type catalysts (see table 24, p. 37). Nevertheless, the surface area of the raw cemented catalyst is still of a relatively low order, about 1 m.²/gm.

RATE OF REDUCTION OF FUSED-IRON CATALYSTS

GENERAL RATE EQUATION

In the previous section on structural changes during reduction of a fused catalyst, it was stated that the reduction appears to proceed uniformly inward from the external surface and that the rate was proportional to the area of the iron-magnetite interface. For simplicity

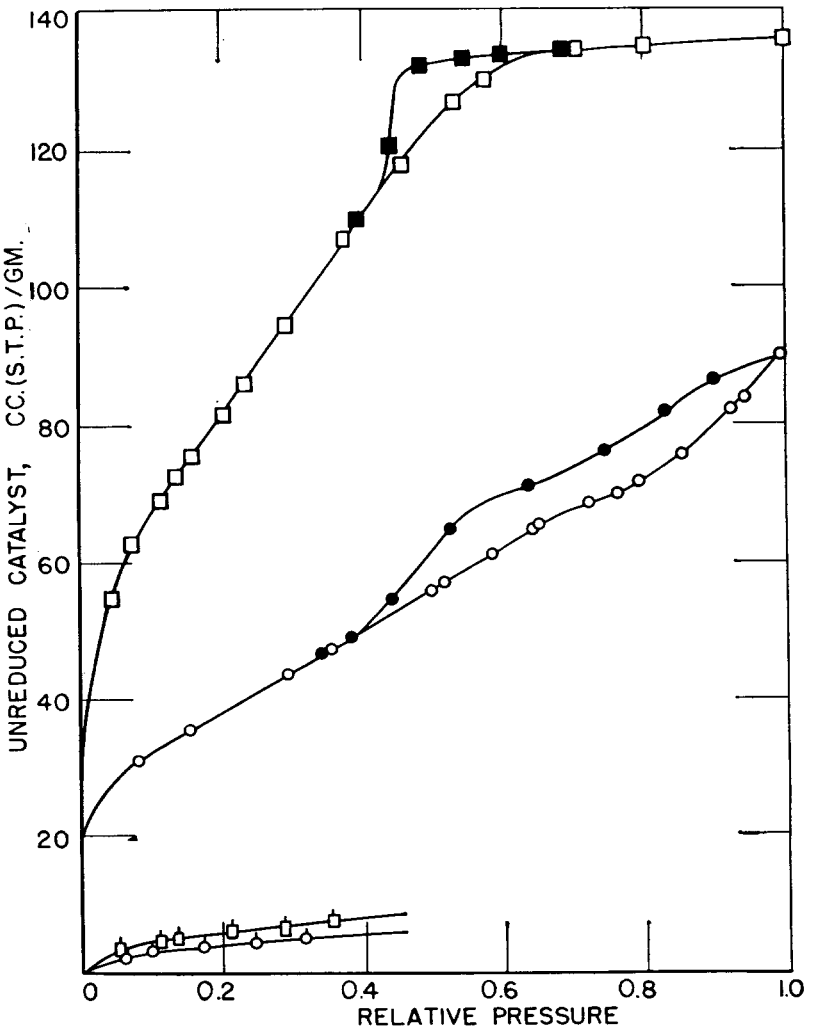

FIGURE 20.—Adsorption Isotherms of Nitrogen on 100Fe : 10Cu : 0.5 K_2CO_3 Catalysts at −195° C.

□, Black catalyst P3003.03, P3003.042, and P3003.05; ○, brown catalyst P3003.07, adsorption points open, desorption points solid. Points with tails represent black and brown catalysts, respectively, after induction in 1 : 1 gas at 230° C.

the particles were assumed to be smooth spheres of radius R. Then

$$-\frac{dV}{dt}=kA, \tag{15}$$

and

$$-\frac{dr}{dt}=k, \tag{16}$$

where V is the volume of catalyst reduced and A and r are the area and radius of the iron-magnetite interface, respectively. On integration and rearranging terms,

$$(1-f)^{1/3}=1-\frac{kt}{R}, \tag{17}$$

where f is the fraction of the catalyst reduced at time t. Equation 15 is presented in a different form in a previous footnote.[96]

[96] Work cited in footnote 82, p. 36.

A plot of data of figure 14 (p. 36) for catalyst D3001 at 450° C. in figure 21 shows that equation 17 accurately depicts the reduction process despite the simplifying assumptions.

CATALYST COMPOSITION AND PARTICLE SIZE

The relative ease of reduction of fused-iron catalysts D3001 (Fe_3O_4-MgO-K_2O), D3004 (Fe_3O_4-Al_2O_3-K_2O), and A3213.24 (cemented Fe_3O_4) is shown in figure 22. In each experiment a 6- to 8-mesh fraction of the catalyst was reduced at 450° C. and a space velocity of hydrogen of 1,000 $hr.^{-1}$ The cemented-magnetite catalyst was 90 percent reduced in about one-seventh of the time required to obtain the same extent of reduction with the usual magnesia-containing catalyst. In the 42-hour period ordinarily used for reduction in testing catalysts, the alumina-containing catalyst was

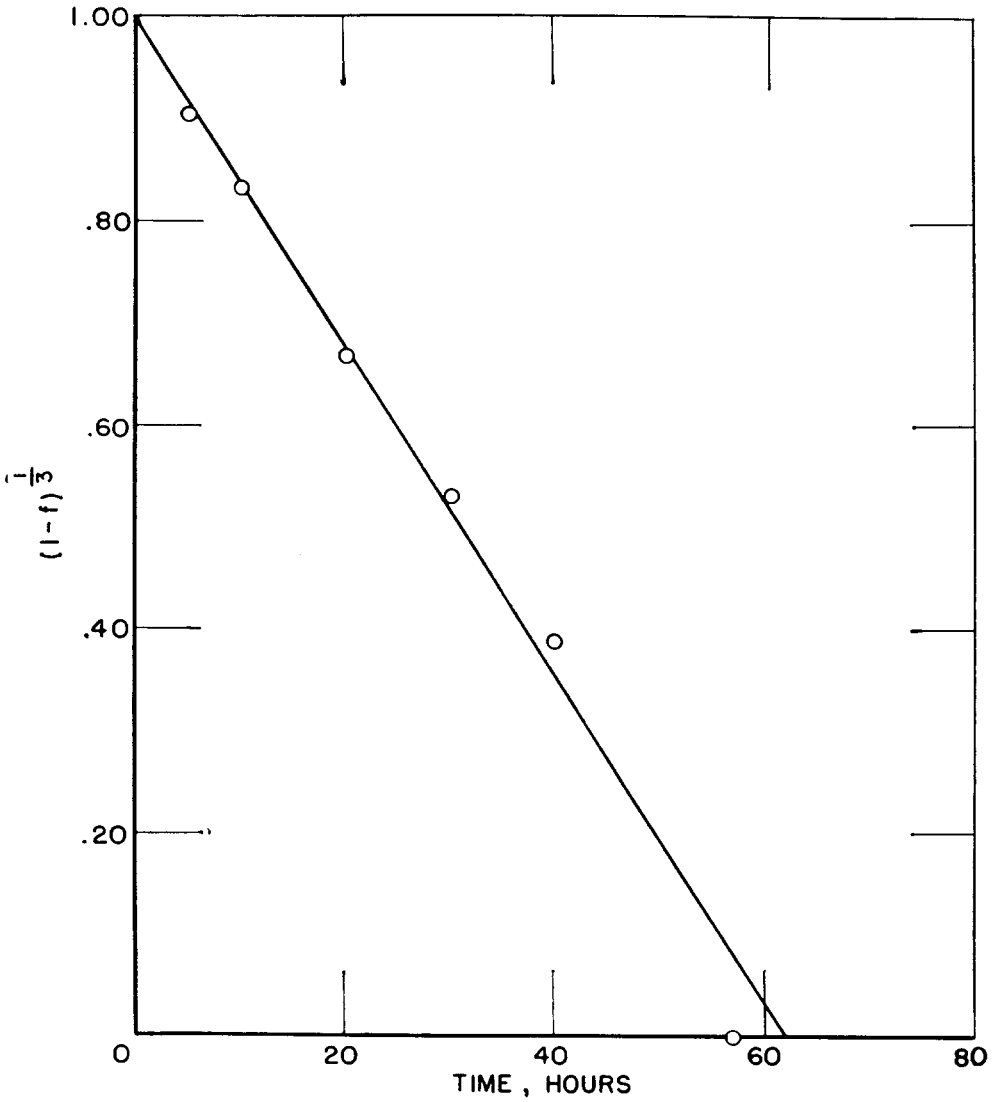

FIGURE 21.—Reduction Data From Figure 14 Plotted According to Equation (17).

only 54 percent reduced, while the other 2 catalysts were nearly completely reduced. The rate of reduction of synthetic-ammonia-type catalyst D3001 at 450° C. was influenced by the particle size of the catalyst. A 14- to 18-mesh fraction reduced more rapidly than a 6- to 8-mesh fraction.

INFLUENCE OF OPERATING VARIABLES

FLOW OF HYDROGEN

The effects of flow rate and pressure of hydrogen on the extent of reduction of fused catalyst D3006 at 450° C. for 12 hours are shown in table 31. The first group of data indicates that linear velocity is no criterion for determining the extent of reduction. Space velocity, however, can be correlated with reduction; according to the second group of data, reduction increased linearly with space velocity up to about 450 volumes per volume-hour and then increased linearly between 450 and 3,424 volumes per volume-hour, but at a slower rate. The third group of data in this table shows that a variation of the hydrogen pressure has little effect on the extent of reduction under otherwise equal conditions.

The rate of reduction of fused-iron catalyst D3001 in pure hydrogen at 550° C. was very much slower at a space velocity of 100 (45 hours for 50-percent reduction) than at 1,000 (6 hours for 50-percent reduction). The results of the experiments (plotted in fig. 23) again suggest that the initial rate of reduction is roughly proportional to the space velocity.

COMPOSITION OF REDUCING GAS

The presence of small amounts of water vapor in the reducing gas decreases the rate of reduction of metal oxides. For this reason,

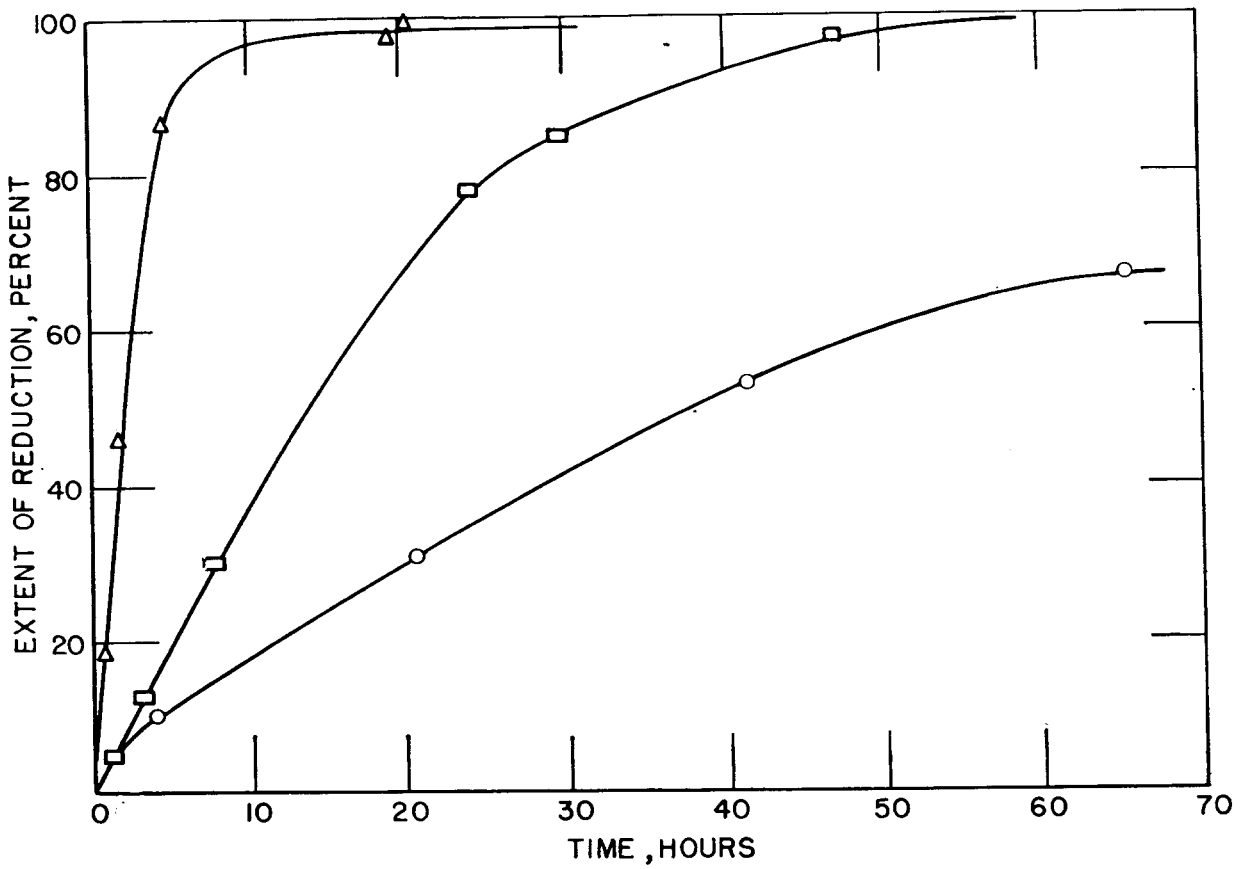

FIGURE 22.—Reduction of Fused-Iron Catalysts at 450°C. and Space Velocity of Hydrogen of 1,000 Hr.$^{-1}$

○, D3004 (Al_2O_3);□,D3001 (MgO);△, A3213.23 (cemented Fe_3O_4).

TABLE 31.—*Effect of pressure and flow rate of hydrogen on reduction of synthetic-ammonia-type catalyst D3006 at 450° C. for 12 hours*

Experiment No.	Pressure, p. s. i. g.	Space velocity, vol. gas × vol. cat.$^{-1}$ × hr.$^{-1}$	Reduction, percent [1]
Constant linear velocity			
RA-71	0	655	26.8
RA-84	50	9,550	73.5
RA-81	100	15,137	90.0
RA-82	200	30,284	88.5
Constant pressure			
RA-67	0	110	5.6
RA-68	0	212	11.2
RA-69	0	335	18.6
RA-70	0	446	24.5
RA-72	0	800	29.1
RA-76	0	1,284	32.1
RA-77	0	2,400	47.1
RA-79	0	3,424	58.0
Constant space velocity			
RA-35	0	2,000	53.4
RA-45	100	2,000	52.0
RA-43	225	2,000	60.2
RA-44	300	2,000	64.4

[1] Based on weight loss.

high space velocities of hydrogen are normally used so that the partial pressure of the water formed by reduction is low. Figure 24 shows that the rate of reduction of fused-iron catalyst D3001 at 450° C. and a space velocity of hydrogen of 1,000 per hour decreased as the moisture content of the hydrogen increased. When dry rather than moist hydrogen was passed over one of these catalysts (point *A* on the curve), the rate of reduction increased immediately to that observed for the catalyst reduced entirely in dry hydrogen to the same extent.

The effect of carbon dioxide in the reducing gas is shown in figure 23. Carbon dioxide was almost twice as effective as water vapor in decreasing the rate of reduction of the same fused-iron catalyst at 550° C. Carbon monoxide also decreased the rate of reduction, but to a smaller extent than water vapor (fig. 25). Methane in the reducing gas had no effect on the reduction rate.

At least part of the carbon monoxide and carbon dioxide in the hydrogen mixture was hydrogenated to methane. Small amounts of

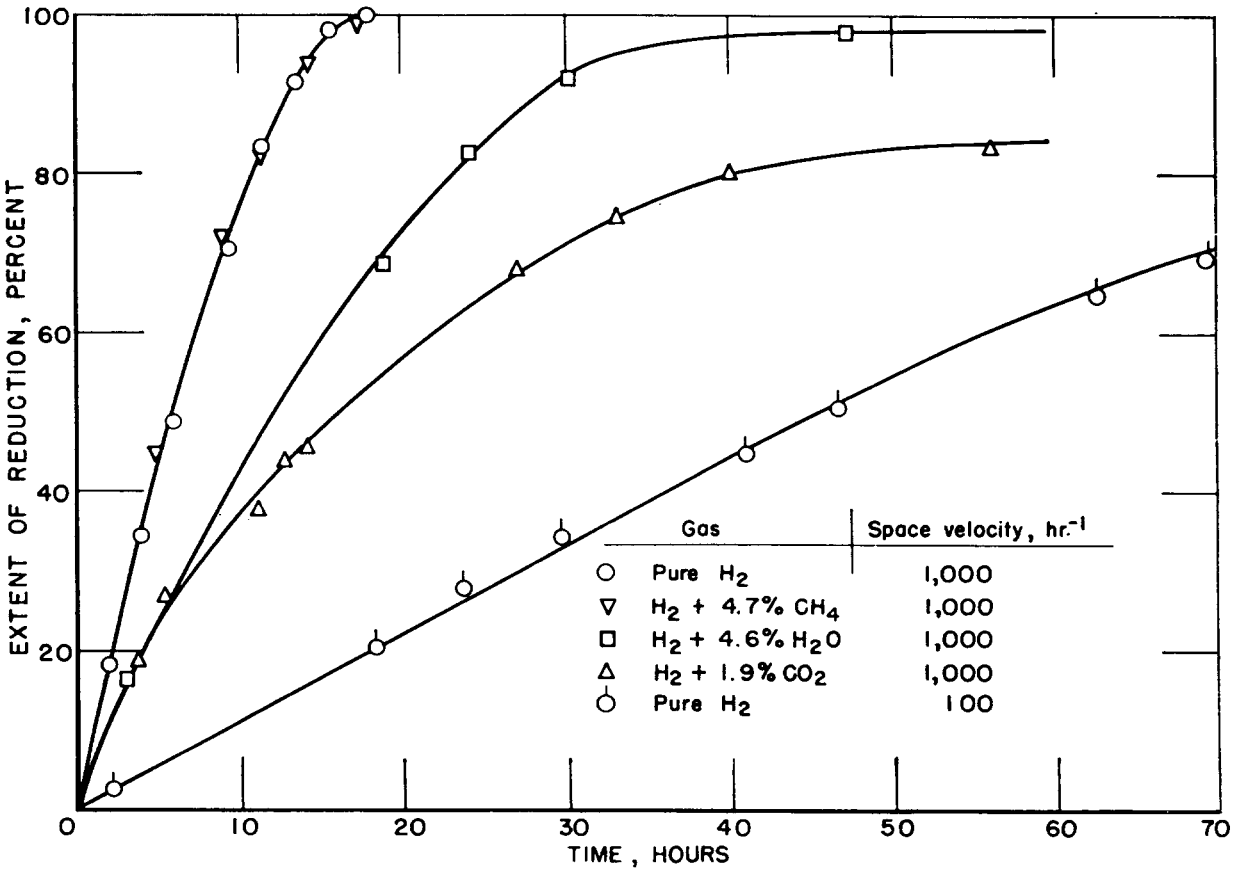

FIGURE 23. — Rate of Reduction of Catalyst D3001 at 550° C. in Pure Hydrogen and in Hydrogen Containing Water, Carbon Dioxide, and Methane.

carbon monoxide were almost completely converted to methane. When hydrogen containing 0.1 percent carbon monoxide, 1.8 percent carbon dioxide, and 4.7 percent methane and saturated with water vapor at 27° C. was used, the carbon dioxide was largely converted to carbon monoxide and, to a smaller extent, to methane at the beginning of the reduction. After reduction for 40 hours, the percentage of carbon monoxide in the exit gas had decreased but was still greater than that present in the inlet gas. These results are summarized in table 32.

TABLE 32.—*Analysis of gas mixtures used in reduction of catalyst D3001, percent*

Gas	Dry gas				Gas saturated with water vapor at 27° C.; at 550° C.		
	At 450° C.		At 550° C.		Inlet	Outlet, after reduction	
	Inlet	Outlet	Inlet	Outlet		2–4 hr.	39–41 hr.
H_2	98.6	98.6	97.9	98.0	93.2	91.4	91.2
CO	1.4	≪.1	1.8	.2	.1	1.2	.3
CH_4		1.1		1.7	4.7	7.4	8.6
CO_2		.3			1.8	.3	.1

TEMPERATURE

Figure 26 shows rate of reduction curves for fused-iron catalyst D3001 at 450° and 550° C. with dry and wet hydrogen. An increase in temperature of 100° C. greatly increased the rate of reduction in both cases. The presence of water vapor decreased the rate of reduction less at 550° than at 450° C. The rate of reduction with wet hydrogen at 550° C. approximately equaled that with dry hydrogen at 450° C. Similar results were obtained with fused-iron catalyst D3004 (6- to 8-mesh) in a 1-foot-deep catalyst bed. Using a space velocity of hydrogen of 2,000 per hour for 24 hours, a 48.5-percent reduction was obtained at 450° C., whereas at 500° C. the reduction obtained was 93.9 percent.

PRESSURE

The effect of pressure on the extent of reduction at constant linear gas velocity of 1.54 ft. per sec. was shown (table 31) for synthetic-ammonia-type catalyst D3006 (4- to 6-mesh) in a series of experiments at 450° C. Optimum reduction took place at about 100 p. s. i. g.,

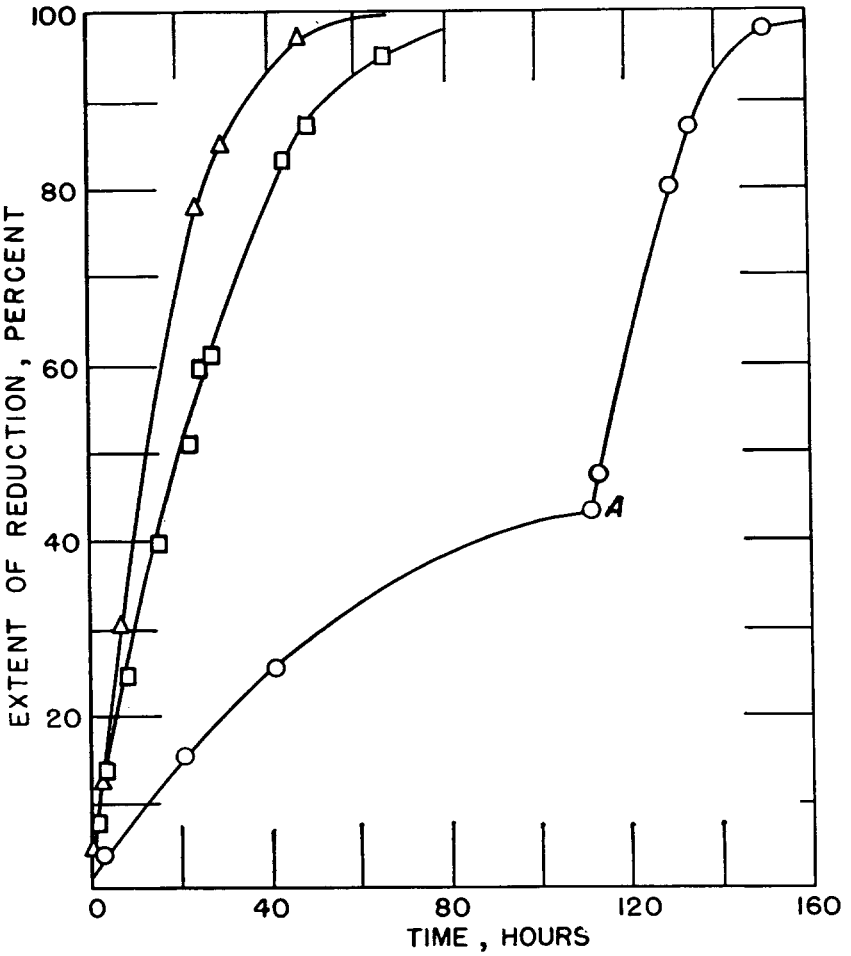

FIGURE 24.—Influence of Water Vapor in Hydrogen on Rate of Reduction of Catalyst D3001 at 450° C. and Hourly Space Velocity of 1, 000.

△, dry H_2; □, H_2 saturated at 0°-2°C., ○, H_2 saturated at 30°-32°C. At point *A* dry hydrogen was passed over catalyst.

and 90-percent reduction resulted. No further advantage was obtained by reducing at 200 p. s. i. g. The effect of pressure on the extent of reduction at constant space velocity (varying linear gas velocity) is also shown in table 31. At 450° C. an increase of 11 percent in extent of reduction resulted from increasing pressure from 0 to 300 p. s. i. g. Thus, the rate of reduction appears to be principally a function of space velocity. The rate increased slightly as pressure was increased at constant space velocity.

IRON CARBIDES

PREPARATION AND IDENTIFICATION

Of the known carbides of iron, 4 have been identified in used iron Fischer-Tropsch catalysts; and as a matter of fact, 2 were first discovered in such catalysts—the hexagonal close-packed carbide [97] and the so-called "FeC".[98] The others are Hägg carbide [99] and the well-known cementite. Identification of these carbides with the Curie points previously reported in carbided-iron catalysts [1] correlated the thermomagnetic studies with the powder-diffraction studies in the literature.[2] The chemical composition of hexagonal carbide corresponds approximately to Fe_2C, at least when the carbide is obtained by carburization of finely divided iron; when obtained from tem-

[97] Group Leader Conference, Ludwigshafen, TOM Reel '26, Bag 2463, Report by Dr. Wenzel, T. O. M. Reel 134, Item II/10. Status of the Synol Problems: April 10, 1942.

[98] Eckstrom, H. C. and Adcock, W. A., New Iron Carbide in Hydrocarbon-Synthesis Catalysts: Jour. Am. Chem. Soc., vol. 72, 1950, pp. 1042-1043.

[99] Hägg, G., Powder Photographs of a New Iron Carbide: Ztschr. Krist., vol .89, 1934, pp. 92-94.

[1] Pichler, H. and Merkel, H., Chemical and Thermomagnetic Studies on Iron Catalysts for Synthesis of Hydrocarbons: Bureau of Mines Tech. Paper 718, 1949, pp. 3-15, 22-25 (108 pp.).

[2] Hofer, L. J. E., Cohn, E. M., and Peebles, W. C., Modifications of the Carbide Fe_2C: Their Properties and Identification: Jour. Am. Chem. Soc., vol. 71, 1949, pp. 189-195.

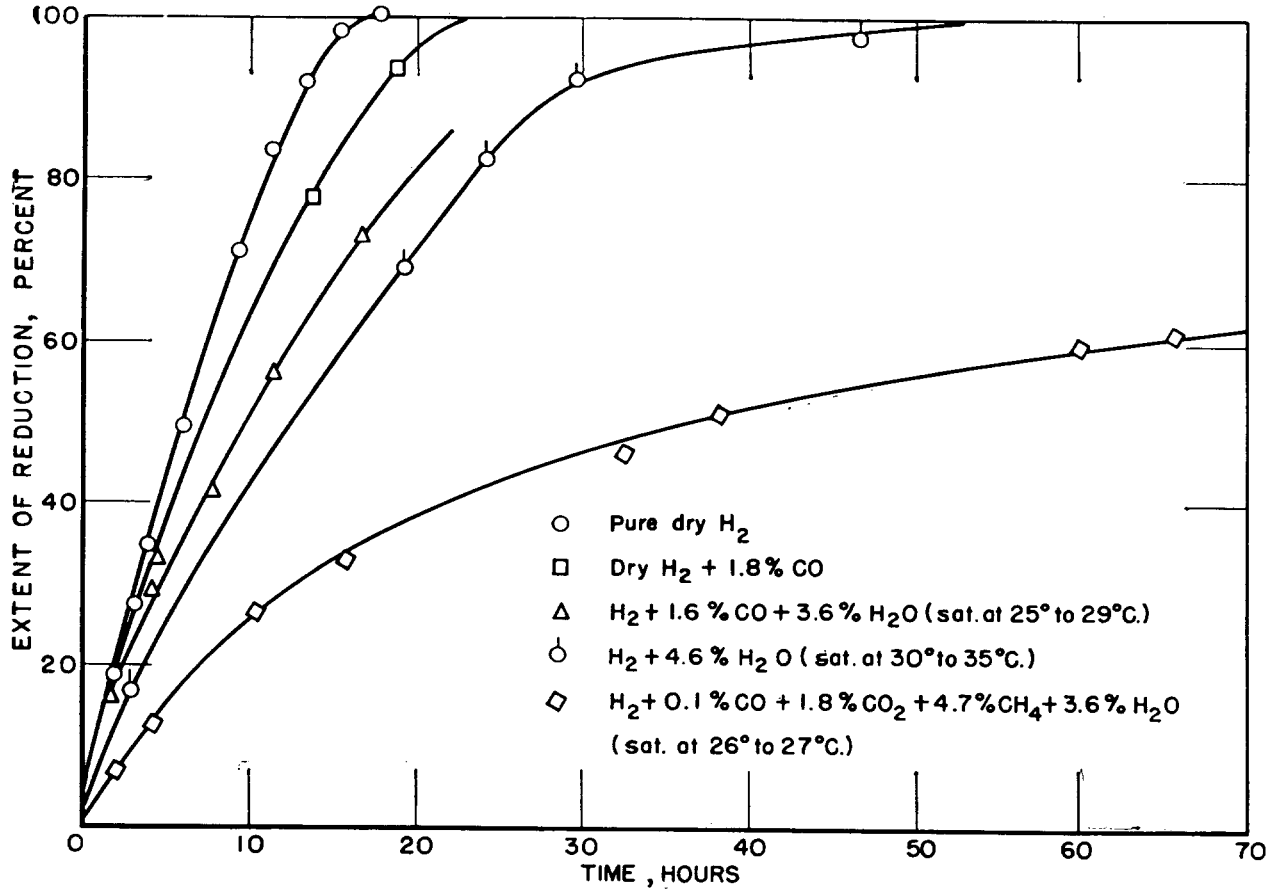

FIGURE 25.—Rate of Reduction of Fused Catalyst D3001 at 550° C. in Pure Dry H_2 and in H_2 Containing Different Amounts of CO, CO_2, CH_4, and H_2O.

pered martensite, its carbon content may be lower.[3] Hägg carbide probably contains somewhat less carbon than Fe_2C.[4] Cementite corresponds closely to the formula Fe_3C. Comparative X-ray diffraction data for the carbides are given in table 33, and their magnetic characteristics are shown in table 34.

The magnetic and perhaps also other properties of Hägg carbide appear to depend on whether iron or iron oxide is used as the raw material. Specimens of Hägg iron carbide have been produced by the direct carburization of iron oxide. These specimens are characterized by a higher Curie point than normal (260°–270° C.) and by a diffraction pattern in which some of the characteristic reflections of normal Hägg iron carbide are either absent or very diffuse. The higher Curie point of this type of carbide may be related to residual oxygen retained in the carbide structure, but this would be difficult to prove. It is also very difficult to establish where oxygen has in fact been retained in the carbide structure. The odd diffraction pattern of these specimens is probably related to a relaxation of the Laue conditions, but this too cannot be established until the crystal structure of Hägg carbide itself is determined. The diffuse reflections may prove to be a clue to the determination of that structure.[5]

Except for "FeC," about which very little is known as yet, the carbides can be prepared by carburizing finely divided iron or iron oxide with carbon-containing gases, especially carbon monoxide. Hexagonal carbide requires a low temperature of carburization (about 170° C. or less when iron is used initially); Hägg carbide can be obtained reasonably pure from reduced iron at temperatures up to about 250° C., although the temperature may be raised considerably at advanced stages of carburization; cementite can be prepared by direct carburization of reduced iron at temperatures exceeding

[3] Jack, K. H., Results of Further X-ray Structural Investigations of the Iron-Carbon and Iron-Nitrogen Systems and of Related Interstitial Alloys: Acta Cryst, vol. 3, 1950, pp. 392-394.

[4] Jack, K. H., Binary and Ternary Interstitial Alloys: Proc. Roy. Soc. (London), vol. A195, 1948, pp. 34-61.

[5] Cohn, E. M., Bean, E. H., Mentser, M., Hofer, L. J. E., Pontello, A., Peebles, W. C., and Jack, K. H., The Carburization of Iron Oxide With Carbon Monoxide; Modifications of Hägg Iron Carbide: Jour. Appl. Chem., vol. 5, 1955, pp. 418-425.

TABLE 33.—*Comparative X-ray diffraction data for cementite, Hägg carbide, hexagonal carbide, and "FeC"*

(1) Cementite					(2) Hägg carbide				(3) Hexagonal iron carbide			(4) "FeC"	
Westgren (calculated)			Bureau of Mines sample 7–68		Hägg		Bureau of Mines sample 7–255		Bureau of Mines sample 8–20			Eckstrom and Adcock	
I	*d/n*	*hkl*	*I*	*d/n*	*I*	*d/n*	*I*	*d/n*	*hkl*	*I*	*d/n*	*I*	*d/n*
					w−	2. 64	vw	2. 62					
					w	2. 49	w	2. 48					
1800	2. 38	112			w+	2. 41	w	2. 39					
1900	2. 37	021	M	2. 37					100		2. 38		
1600	2. 26	200	w	2. 25	M	2. 27	M	2. 26				35	2. 250
					vw	2 24							
1400	2. 18	120	w	2. 18	M	2. 20	M	2. 18					
					w	2. 18							
									200	M	2. 16		
3800	2. 10	121	w	2. 10	w+	2. 10						45	2. 115
3800	2. 06	210	M	2. 06	S	2. 07	vS	2. 06	101	vS	2. 08		
3500	2. 02	022			S	2. 04	vS	2. 03					
6300	2. 01	103	vS	2. 01	w	2. 01						100	2. 012
					w	2. 00							
3700	1. 97	211	M	1. 97	w	1. 97	1 w	1. 98					
					w+	1. 91	M	1. 91					
3400	1. 87	113	M	1. 87									
4200	1. 85	122	M	1. 85									
					M	1. 81	S	1. 80				30	1. 801
					w	1. 76	vw	1. 76					
					1 w	1. 72	vw	1. 72					
												15	1. 716
430	1. 68	004											
1100	1. 68	023	w	1. 68	1 w	1. 68	vw	1. 67					
					1 vw	1. 625							
					vw	1. 623	vw	1. 62					
									102	M	1. 60		
1600	1. 58	130	w	1. 58	M	1. 57	S	1. 57					
950	1. 51	222											
240	1. 51	114	w	1. 51	w	1. 51	vw	1. 50					
					w	1. 47							
					w	1. 41							
510	1. 401	024	vw	1. 403									
					w	1. 38	vw	1. 37	110	M	1. 37		
					w	1. 33	vw	1. 34				15	1. 346
6200	1. 324	312	M	1. 322	w	1. 32	vw	1. 32					
					1 w	1. 27	w	1. 27					
					w	1. 25	w	1. 25	103	M	1. 24		
3200	1. 219	140	M	1. 222									
400	1. 211	313	M	1. 214									
					S	1. 21	M	1. 21					
580	1. 200	141			w	1. 20						35	1. 201
280	1. 190	224	M	1. 189	1 w	1. 19	w	1. 17					
4800	1. 157	233	S	1. 159	1 w	1. 16	w	1. 16	112	M	1. 16	30	1. 167
190	1. 152	134							201				
540	1. 148	125											
170	1. 146	142	M	1. 149	M	1. 15	w	1. 14				25	1. 149
750	1. 127	400										25	1. 144
3500	1. 126	215											
4600	1. 122	330											
2300	1. 121	006	S	1. 124	S	1. 12	M	1. 13				10	1. 128
4800	1. 102	043	S	1. 104	1 w	1. 10	1 w	1. 11				10	1. 112
2000	1. 094	314	vw	1. 096									
					1 w	1. 08	1 w	1. 09					
1800	1. 085	411	vw	1. 087									
2000	1. 050	225											
1100	1. 045	412	w	1. 052									
1400	1. 017	421	vw	1. 002									
1500	1. 003	206	w	. 992									
6800	. 991	213	1 M	. 986									

vS=very Strong, S=Strong, M=Medium, w=weak, vw=very weak, +=slightly more intense, −=slightly less intense. 1 Broad.